X-612-69-156
PREPRINT

MAGNETOMETERS FOR SPACE MEASUREMENTS OVER A WIDE RANGE OF FIELD INTENSITIES

B. G. LEDLEY

MAY 1969

GSFC
GODDARD SPACE FLIGHT CENTER
GREENBELT, MARYLAND

MAGNETOMETERS FOR SPACE MEASUREMENTS OVER A WIDE RANGE OF FIELD INTENSITIES

by

B. G. Ledley

May 1969

NASA Goddard Space Flight Center
Greenbelt, Maryland 20771

[TO BE PUBLISHED IN THE PROCEEDINGS OF THE URSI CONFERENCE ON "WEAK MAGNETIC FIELDS OF INTEREST IN GEOPHYSICS AND SPACE" TO BE HELD IN PARIS IN MAY 1969]

PREAMBLE

One of the many by-products of space research has been the rapid development of magnetometry in the past decade. Many spacecraft explore both magnetospheric and interplanetary regions; this has emphasized the development of magnetometers capable of measuring over a wide range of field intensities.

This paper will discuss some of the wide range magnetometers developed by the Goddard Space Flight Center. The Center's magnetic field experiment flown on the fifth Orbiting Geophysical Observatory (OGO-5) contains both a Rubidium vapor magnetometer and a triaxial fluxgate with a digitally controlled field compensation system. These magnetometers and current development at Goddard Space Flight Center (GSFC) of these two types of magnetometers are described below.

RUBIDIUM VAPOR MAGNETOMETER

(1) Introduction

The development of optical pumping techniques arose from the suggestions in 1949 of F. Bitter [1] and of J. Brossel and A. Kastler [2] for a double resonance technique to detect the radiofrequency resonances of optically excited states of atoms. Observations of the orientation of atoms by optical pumping, both in atomic beams and saturated vapor, followed [3]. In 1957 H. G. Dehmelt [4] pointed out that atomic precession could be observed by the resulting modulation of the transmitted light beam. He also proposed a self-oscillating device. In the same year W. E. Bell and A. L. Bloom [5]

developed a model of double resonance phenomena and they suggested the application of optical pumping methods to the measurement of weak magnetic fields. In 1958 the first optical pumping magnetometer was constructed [6] and in 1961 the space probe Explorer 10 carried a self-oscillating Rubidium magnetometer [7].

Experiments using optical pumping magnetometers have also been carried on the first three Interplanetary Monitoring Platforms (IMP 1, 2, and 3) [8]. Mariner 4, launched in 1964 carried a "low-field" Helium magnetometer [9]. The Orbiting Geophysical Observatories (OGO 1, 2, 3, 4, and 5) have all included Rubidium vapor magnetometers [10,11]. W. H. Farthing and W. C. Folz [11] have published a detailed description of the Rubidium vapor magnetometer experiments carried on the Polar Orbiting Geophysical Observatories (OGO 2 and 4). Those two experiments and the spacecrafts involved had many similarities to their OGO-5 counterparts. The discussion below is not a complete description of the OGO-5 experiment; rather it is a description of some of the features peculiar to the OGO-5 magnetometers.

(2) <u>OGO-5</u>

The orbit of OGO-5 is highly eccentric; apogee is approximately 22 earth radii above the earth's surface and perigee was initially 290 kilometers. The corresponding magnetic fields range from typical interplanetary fields of a few gammas up to maximum magnetospheric intensities in excess of forty thousand gammas.

Figure 1 shows the configuration of OGO-5. The Rubidium magnetometer's sensor is housed in a sphere at the end of a six meter boom shown in the right side of the figure. The lamp oscillators are located approximately one-half meter inboard and the triaxial fluxgate sensor about two meters inboard from the sphere.

Two dual gas cell Rb^{87} magnetometers are combined and phase-locked to form an OGO-5 magnetometer. Their optical axes subtend an angle of 45°. As discussed previously [10], this combined configuration minimizes errors due to misalignment of the optical axis with the H1 coil axis and reduces the dead zones by an order of magnitude below that of a single magnetometer. Figure 2 is a block diagram of one of the two dual cell units.

The level of the H1 field is fixed by a clipper circuit on the output of each amplifier and a resistance in series with each H1 solenoid. The solenoidal field is thus a square wave; the peak-to-peak value of this is set at 2.5 gammas, corresponding to an amplitude of 0.8 gamma for the desired rotating component at the fundamental frequency. One of the practical limitations on the choice of magnitude of the H1 field is the "squegging" which is observed in weak fields if the H1 field is comparable in magnitude for the ambient field. This effect has been previously reported and analyzed [12,13].

The lamp circuit has a feedback loop containing a monitoring photocell, the amplified output of which controls the lamp oscillator power level. When preparing the magnetometer for flight, the light level is reduced until operation at frequencies below 20 hertz (one gamma $\approx$ seven hertz) is readily obtainable. If the line width is measured at a given light level, it is found in practice that this width is approximately equal to the lowest frequency at which self-oscillation is obtained. This is to be expected under high loop gain conditions, because the expression for the self-oscillating frequency tends asymptotically to the line width as the field is reduced.

$$\nu = ([1/(2\pi T_2)]^2 + \nu_0^2)^{\frac{1}{2}}$$

where $1/(2\pi T_2)$ = the line width in hertz and ν_0 is the frequency for zero line width [12]. Thus, if the line width were 15 hertz, the observed frequency in a three gamma field would be 4.5 hertz higher than ν_0 and in a ten gamma field, 1.5 hertz. If the line width is known the measured frequencies can be corrected.

The length of the boom cabling (approximately 10m) imposes some technical problems. The photocell to amplifier cable capacitance is similar to the photocell's self-capacitance. A non-magnetic preamplifier is used at the photocell to decouple it from the cable capacitive load. The low output impedance of the preamplifier also attenuates low frequency noise picked up on the cable.

The phase delay in this cabling is significant at the high end of the magnetometer's range. Phase delay is important to the operation of the magnetometer, because it affects the self-oscillating frequency. This may be seen as follows: each absorption cell of the magnetometer may be regarded as a "black box", the input being the H1 drive current and the output being the photocell current. The phase-frequency characteristic of the black box is similar to that of a resonant circuit. Since the total phase shift around the magnetometer loop must be zero, the frequency of operation is such that the cable delay and other electronic phase shifts must be exactly cancelled by phase shifts in the black box. Twenty meters of cable are involved in each half of a dual cell magnetometer. At 350 KHz (0.5 Gauss) this gives a phase delay of approximately 10 degrees. In addition, there is an electronic phase lag in the preamplifier-amplifier combination, which is also approximately ten degrees. Many measurements of absolute accuracy of the OGO-5 magnetometers have been made by comparison with a proton magnetometer. Measurements have been made with several field orientations, although no measurements were made within ten degrees of a dead zone when a single dual cell magnetometer was being tested. The maximum error observed with the individual dual cell magnetometers was 15 cps at 350 KHz. (Two coupled dual cell magnetometers, as flown, gave a maximum error of 10 hz, in any orientation.) Although the phase shift between the H1 and photocell signals through resonance was not measured for the OGO-5 magnetometers, it is clear from the above figures that the slope of the phase-frequency plot at the operating part of the resonance curve is ≥ 1.3 degrees per hertz at 0.5 Gauss in any orientation.

(3) Recent Development Work

Goddard Space Flight Center is developing improvements in optical pumping magnetometers for space flight. Figure 3 shows an OGO-5 dual cell magnetometer beside a more recent model. The respective weights of the sensors are 650g and 360g and of the amplifiers 320g and 45g. The cross-sectional area of the present gas cells is one-quarter that of the OGO-5 cells, and this reduces the optical signal in approximately the same proportion for a given light intensity in the gas cell. The signal-to-noise has on balance been increased however, due to other changes which have been made. The first stage of the preamplifier employs a low noise field effect transistor; the capacitance of the photocell has been reduced by a factor of approximately 15 by reducing its surface area and employing a lower capacitance per unit area material. The light reflected back into the gas cell has been reduced by eliminating the final Fresnel lens and instead making the back face of the gas cell into a lens. The sensor optics have also been more accurately defined by providing small apertures on each side of the lamp, dimensioned to match the image sizes to the photocells.

The circuit phase shifts have been reduced. The main amplifier has been made much less magnetic, and capable of operating over a wider temperature range. This enables one to operate them outside the main body of the spacecraft and as close to the sensor as 0.5 meters, which would be equivalent to a phase shift of about one-half

degree at 350 Kc/s. The bandwidth of the electronics has been increased, reducing this phase shift to about five degrees at 350 Kc/s. These phase shifts will, of course, be reduced if Cesium, with its lower precession frequency, is used instead of Rb^{87}.

FLUXGATE MAGNETOMETER

(1) Introduction

The triaxial fluxgate magnetometer system flown on the GSFC OGO-5 experiment employs digitally controlled compensation fields. A block diagram of one axis is shown in Figure 4. Each fluxgate sensor is inside a solenoid which applies the digitally controlled compensation field. This solenoid and compensation system are in addition to, and electrically separate from the analog feedback compensation system of the fluxgate, which determines its sensitivity [14]. The logic of operation is as follows: When the ambient field changes so that the fluxgates D.C. voltage approaches its upper or lower limits, the gate shown opens, permitting the counter to increase or decrease by one count when a pulse is received from the oscillator. The counter controls the digital-to-analog converter, the output current of which determines the compensation field magnitude. The new value of compensation field will cause the fluxgate voltage to return closer to mid-scale, thus shutting the gate until ambient field changes initiate the cycle again.

The ambient field B is given by the number N in the counter and the fluxgate's analog output V by an equation of the form:

$$B = C(N - N_o) + S(V - V_o) \qquad (1)$$

where C is the change in the compensation field when the number in the counter changes by one. N_o is the number in the counter corresponding to zero compensation field. S is the sensitivity of the fluxgates and V_o is the voltage of the fluxgate output which corresponds to zero field.

As in the case of the optical pumping magnetometers, space applications have accelerated the development of this type of system. The first magnetic field experiment flown on a satellite was on Sputnik 3, and it contained a digitally compensated fluxgate [15]. The digital compensation system has been further developed and applied in the magnetic field experiment on ATS-B, in the University of California at Los Angeles hydromagnetic wave experiment on OGO-5, and in the Goddard Space Flight Center magnetic field experiment, also on OGO-5 [16,17].

(2) <u>OGO-5</u>

The Goddard Space Flight Center's experiment utilizes an actively controlled current source in the digital-to-analog converter. This has a very high dynamic D.C. output impedance, which eliminates the problem of changes in the load resistance of the solenoid and boom wires with temperature. The counter in the

experiment controls the selection and switching of reference resistors into the output line of the current source. The voltage drop across these resistors is compared with that of a Zener diode whose current is set for minimum T_c. The comparison is made by a high gain differential amplifier which controls the output current. The operating temperature range of the OGO-5 sensor is from -150°C to +50°C and of the electronics from -5°C to +45°C. The current source and its associated logic and telemetry readout system consumes 0.75 watts of regulated power. The total fluxgate system power is less than 1.5 watts regulated.

The fluxgates have a range of $\pm$ thirty-three gammas; the compensation threshold points are set to keep the sensor in a $\pm$ twenty gamma range. The total range of the system is $\pm$ four thousand gammas. The sensitivity of the fluxgates shows a slight temperature dependence. Over the total range of temperatures given above, this is equivalent to a $\pm$0.5 gamma variation at twenty gammas. The sensitivity is monitored in flight by periodically applying an accurate ten gamma calibration field to each sensor via a secondary solenoid, built into the sensor housing. Apart from this temperature dependence, the system has a calibration over the whole field and temperature range which can be represented to an accuracy of 0.1% $\pm$0.25 gamma by an equation of the form of (1) with constant parameters. The resolution of the measurements is $\pm$1/8 gamma.

(3) Recent Development Work

Development of a more accurate system has been started. The design goal is to measure field components up to 60,000 gammas to an accuracy of 0.01%. This magnetometer would be flown on a low altitude satellite with either 3 axis stabilization or low angular rotation rates and so for design purposes moderately severe thermal conditions are assumed. For example, if only passive thermal conditions are used on the boom mounted sensor, it might be expected to experience a temperature range of $\sim 100^{\circ}C$. The operating range of the electronics is designed to be $-5^{\circ}C$ to $+45^{\circ}C$.

This development is not complete. However, many of the design problems have been solved.

(a) Electronics

A current source has been designed and breadboarded. Among the design features related to the high accuracy are the following: comparison of the Zener voltage with the voltage across the reference resistors is made by means of a chopper-amplifier, rather than the differential amplifier used on OGO-5; the switching of the reference resistors and connection to the chopper amplifier is made by low impedance field effect transistors, whereas bipolar devices were used in OGO-5. The reference resistors and Zener diode are in a thermostatically controlled oven.

Measurements on the breadboard unit over a period of eighty days show the current source to have an accuracy of $\pm$.005% over the specified temperature range. The power requirement of a three-axis unit is two watts, made up of one watt of regulated power for the current sources, logic and telemetry readout, and a watt of unregulated power for the oven. This circuit was designed two years ago; subsequent improvements in component stability would now not require the use of an oven. A three-axis unit could now be designed which would require only 0.8 watts of regulated power.

(b) Structure

The sensor and solenoid mounting structure presented a materials problem from the point of view of stability and thermal coefficient of expansion. To define the field vector to .01% requires a sensor directional stability of the order of twenty seconds of arc. In addition, the compensation field of a long solenoid is proportional to the number of turns per unit length and varies with temperature as the solenoid's length varies. Assuming a 100°C temperature range, the coefficient of linear expansion of the solenoid's structural material should be $< 1 \times 10^{-6}$ per degree centigrade, in order to maintain the overall system accuracy of .01%. Quartz has the desired rigidity for directional stability and has a low coefficient of expansion. However, it is weak in tension and is very difficult to fabricate. A choice was made of CER-VIT, a ceramic vitreous material developed by Owens Illinois, Inc. This material is stronger in tension than quartz and is much easier to fabricate to close tolerances.

In this structure each fluxgate is inside a pair of coaxial solenoids whose fields are in opposition. By a suitable choice of diameter of the two solenoids and of their number of turns per unit length, the external field of the combination can be made to cancel at the locations of the other two fluxgates. This design enables one to locate the three fluxgates close together with minimum interaction.

Thermal testing of fluxgates in short solenoids showed that the expansion and contraction of the active volume of the fluxgate in the high gradient end fields of the solenoids can lead to significant changes in the effective coil constant of the solenoid. To overcome this, a first order correction to the end fields was made by using different lengths for the two opposing solenoids. Figure 5 shows a plot of the on-axis field for a single solenoid and a corresponding plot for the dual solenoids. Both the external field at the location of the orthogonal sensors, and the field gradient over the length of the internal sensor are reduced by an order of magnitude by use of the dual solenoids. Figure 6 shows a preliminary model of the structure which is presently being tested.

The above description has considered only the technical problems of the fluxgate system. When the fluxgate is used on a satellite, the accuracy of determination of the satellite's location and attitude enter into the accuracy of the experiment. The requirements on determination of the satellite's location are comparable with those for the

Polar Orbiting Geophysical Observatories, two of which have already been flown. Determination of the attitude of a slowly rotating satellite to the required accuracy has not yet been accomplished, however the state of the art of star sensors would now permit the development of such a system.

REFERENCES

[1] The Optical Detection of Radiofrequency Resonance, F. Bitter, Phys. Rev., 76, 833, 1949.

[2] La Detection de la Résonance Magnetique des Niveaux Excités: l'effet de Dépolarisation des Radiations Optique et de Fluorescence, J. Brossel and A. Kastler, Compt. Rend., 229, 1213, 1949.

[3] Optical Methods of Atomic Orientation and of Magnetic Resonance, J. Brossel and F. Bitter, Phys. Rev., 86, 308, 1952.

[4] Modulation of a Light Beam by Precessing Absorbing Atoms, H. G. Dehmelt, Phys. Rev., 105, 1924, 1957.

[5] Optical Detection of Magnetic Resonance in Alkali Metal Vapor, W. E. Bell and A. L. Bloom, Phys. Rev., 107, 1559, 1957.

[6] Measurement of the Earth's magnetic Field with a Rudidium Vapor Magnetometer, T. L. Skillman and P. L. Bender, J. Geophys. Res., 63, 513, 1958.

[7] Explorer 10 Magnetic Field Measurements, J. P. Heppner, N. F. Ness, C. S. Scearce, and T. L. Skillman, J. Geophys. Res., 68, 1-46, 1963.

[8] Initial Results of the IMP-1 Magnetic Field Experiment, N. F. Ness, C. S. Scearce, and J. B. Seek, J. Geophys. Res., 69, 3531, 1964.

[9] Measurements of Magnetic Fields in the Vicinity of the Magnetosphere and in Interplanetary Space: Preliminary Results from Mariner 4, P. J. Coleman, Jr., E. J. Smith, L. Davis, Jr., and D. E. Jones, Space Res., 6, 907, 1966.

[10] OGO-A Magnetic Field Observations, J. P. Heppner, M. Sugiura, T. L. Skillman, B. G. Ledley, and M. Campbell, J. Geophys. Res., 72, 5417, 1967.

[11] Rubidium Vapor Magnetometer for Near Earth Orbiting Spacecraft, W. H. Farthing and W. C. Folz, Review of Scientific Instruments, 38, 1023, 1967.

[12] Principles of Operation of the Rubidium Vapor Magnetometer, Arnold L. Bloom, Applied Optics, 1, 61-68, 1962.

[13] General Analysis of Optical, Infrared, and Microwave Maser Oscillator Emission, J R. Singer and S. Wang, Phys. Rev. Letters, 6, 351-354, 1961.

[14] Magnetic Amplifier Circuits: Basic Principles, Characteristics, and Applications, W. A. Geyger, pp. 196-198 (published McGraw-Hill, 2nd Edition, 1957).

[15] Magnetometers in the Third Soviet Earth Satellite, S.Sh. Dolginov, L. N. Zhuzgov, and V. A. Selyutin, Artificial Earth Satellites, 4, 358-396, 1961.

[16] A Fluxgate Magnetometer for the Applications Technology Satellite, J. Dale Barry and Robert C. Snare, IEEE Transactions on Nuclear Science, NS-13, 326-332, 1966.

[17] A Magnetic Field Instrument for the OGO-E Spacecraft, R. C. Snare and C. R. Benjamin, IEEE Transactions on Nuclear Science, NS-13, 333-339, 1966.

ACKNOWLEDGMENTS

The instruments described have been the responsibility of several members of GSFC, not that of the author only.

Among the companies which contributed to the OGO-5 experiment development are the Matrix Research and Development Corporation, the Schonstedt Instrument Corporation, and Varian Associates. The mechanical design and fabrication of the CER-VIT structure to meet the GSFC vibration specifications is being performed by Owens-Illinois, Inc.

FIGURE CAPTIONS

1. The OGO-5 Spacecraft. The Rubidium vapor magnetometer sensor is housed in the striped sphere on the end of the right-hand boom; the fluxgate sensor is located one-third of the way inboard on the same boom.

2. Block diagram of a dual-cell rubidium magnetometer. The OGO-5 experiment contains two of these magnetometers.

3. Comparison of one of the dual-cell OGO-5 magnetometers with a recently developed unit.

4. Block diagram of a fluxgate with a digitally controlled compensation system.

5. Plots of the axial fields of a single solenoid and of a coaxial pair of solenoids with opposing field vs. the axial distance from the center. The shaded area, Sensor 1, gives the location of the sensor inside the solenoid. The two orthogonal sensors are located 8 cm from the center of the Sensor 1 solenoid, and are indicated by the other shaded area.

6. A triaxial compensation system made of CER-VIT.

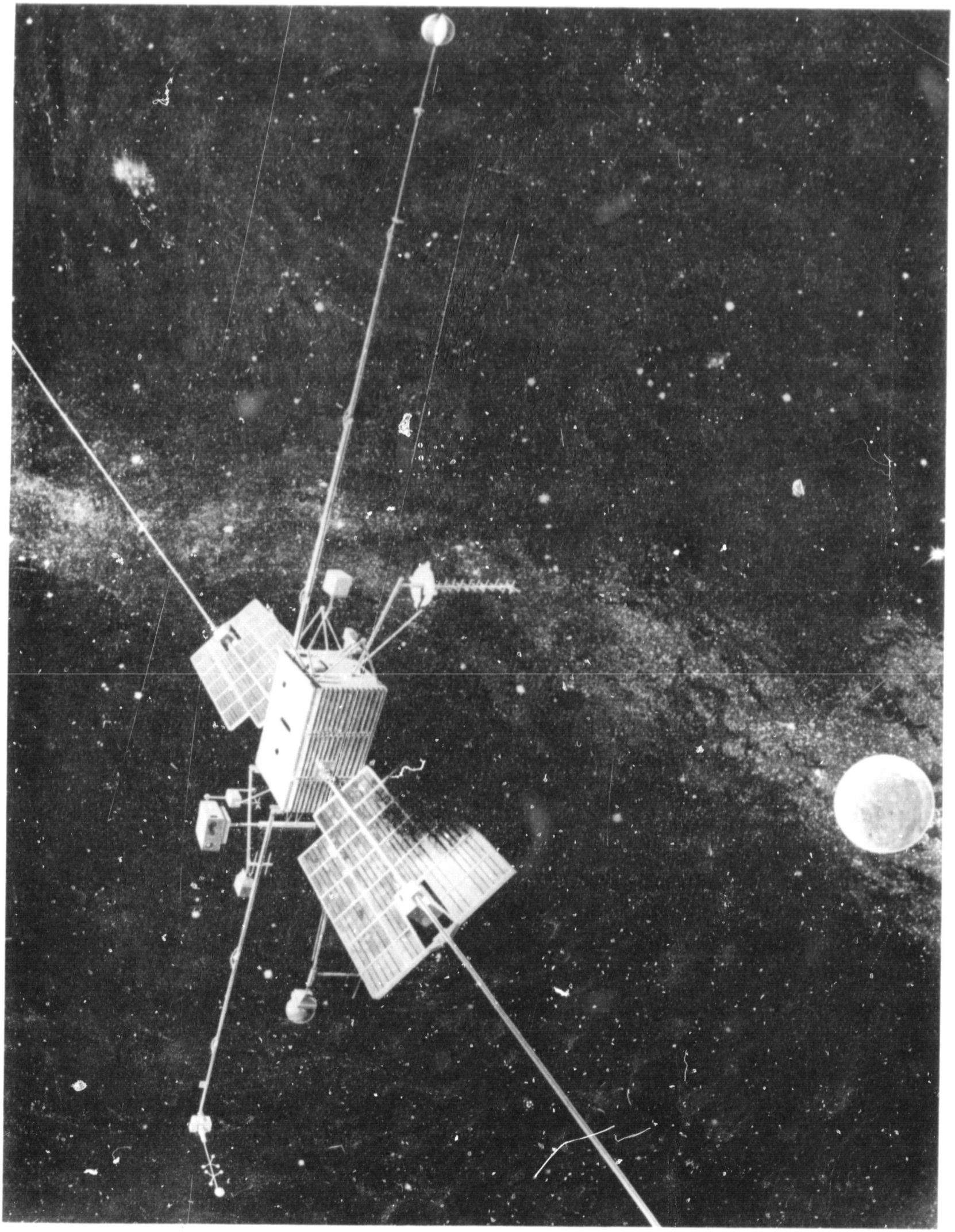

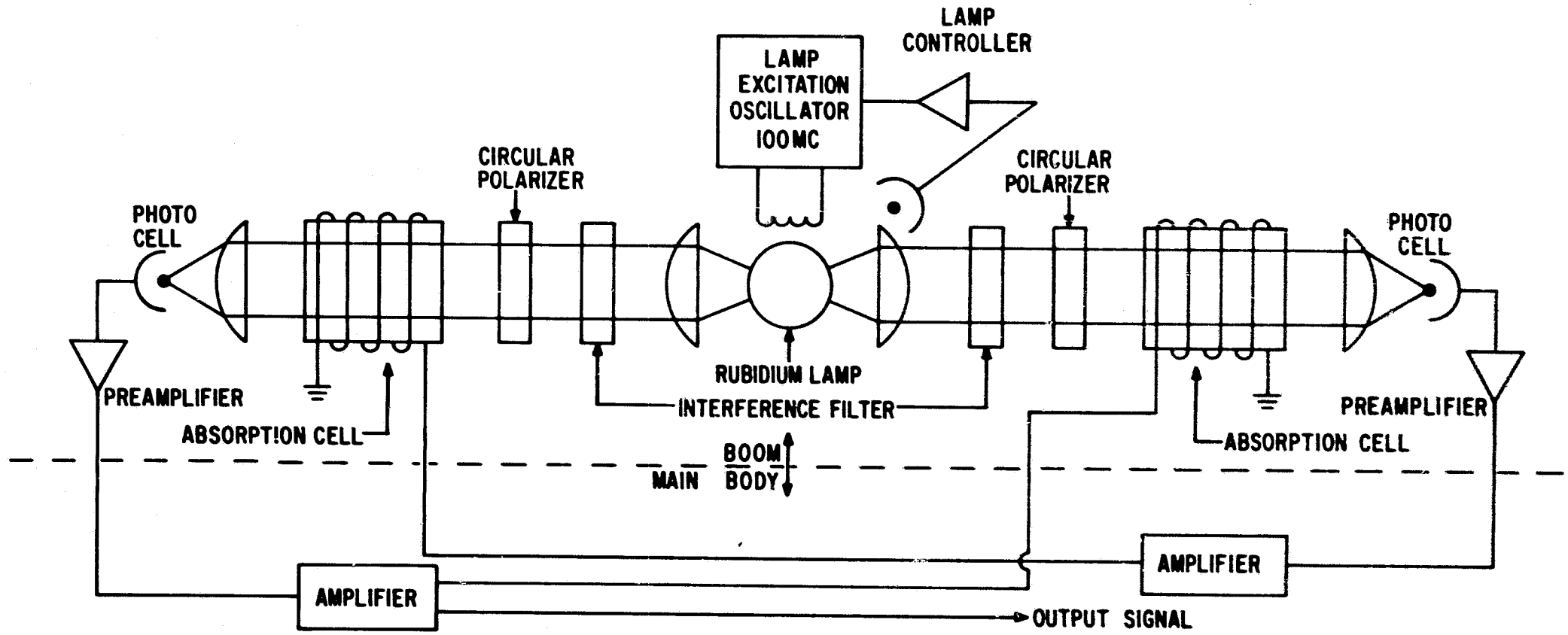
LAMP
CONTROLLER
LAMP
EXCITATION
OSCILLATOR
100MC
CIRCULAR
POLARIZER
CIRCULAR
POLARIZER
PHOTO
CELL
PHOTO
CELL
RUBIDIUM LAMP
INTERFERENCE FILTER
PREAMPLIFIER
ABSORPTION CELL
BOOM
MAIN BODY
ABSORPTION CELL
PREAMPLIFIER
AMPLIFIER
AMPLIFIER
OUTPUT SIGNAL

OGO 5

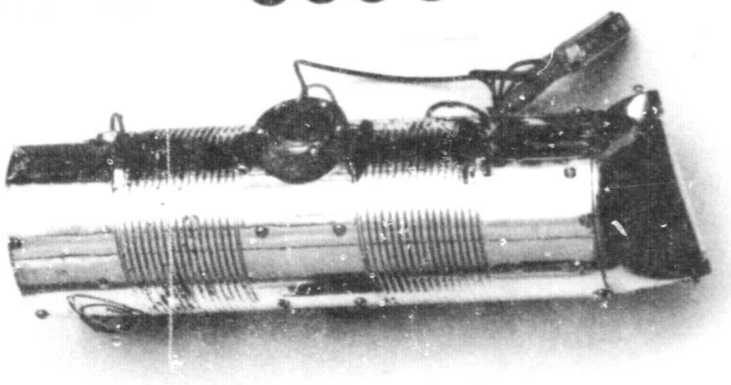

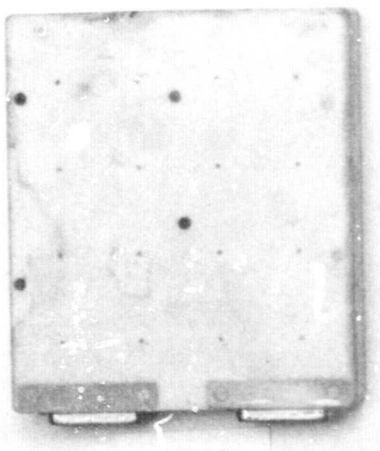

1.05Kg

DEVELOPMENT

SENSORS

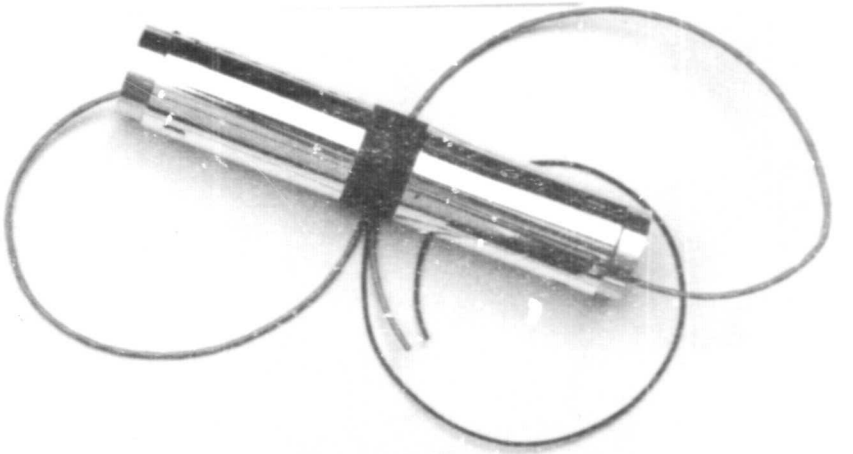

LAMP OSCILLATORS

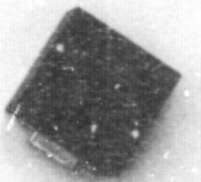

AMPLIFIERS

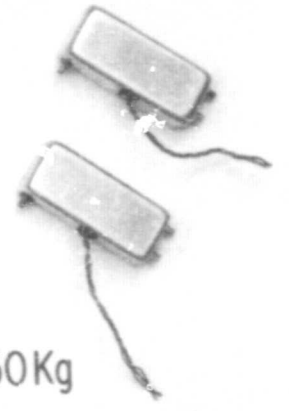

.50Kg

TOTAL WEIGHTS

6 INCHES

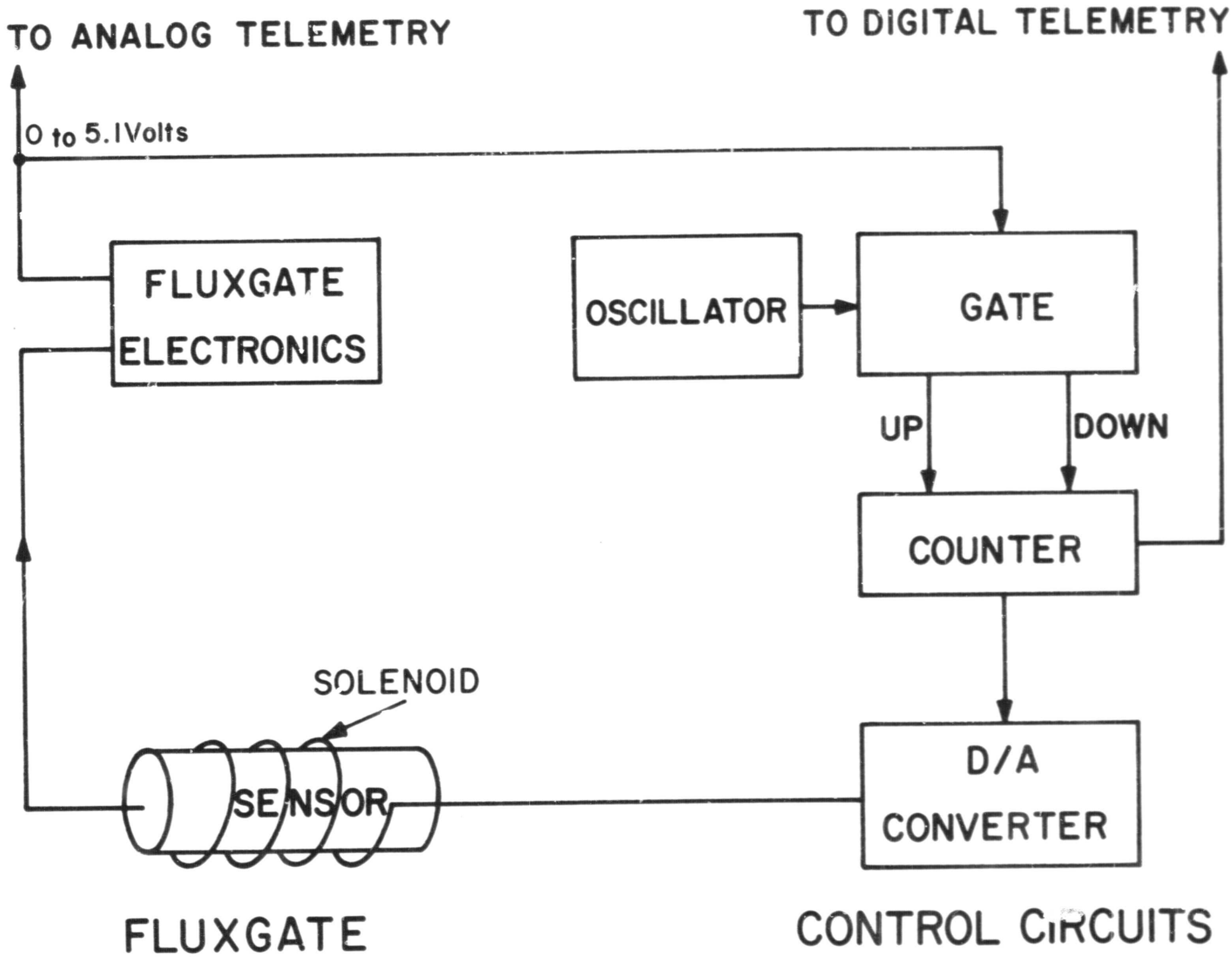
TO ANALOG TELEMETRY
TO DIGITAL TELEMETRY
0 to 5.1Volts
FLUXGATE
ELECTRONICS
OSCILLATOR
GATE
UP
DOWN
COUNTER
D/A
CONVERTER
SOLENOID
SENSOR
FLUXGATE
CONTROL CIRCUITS

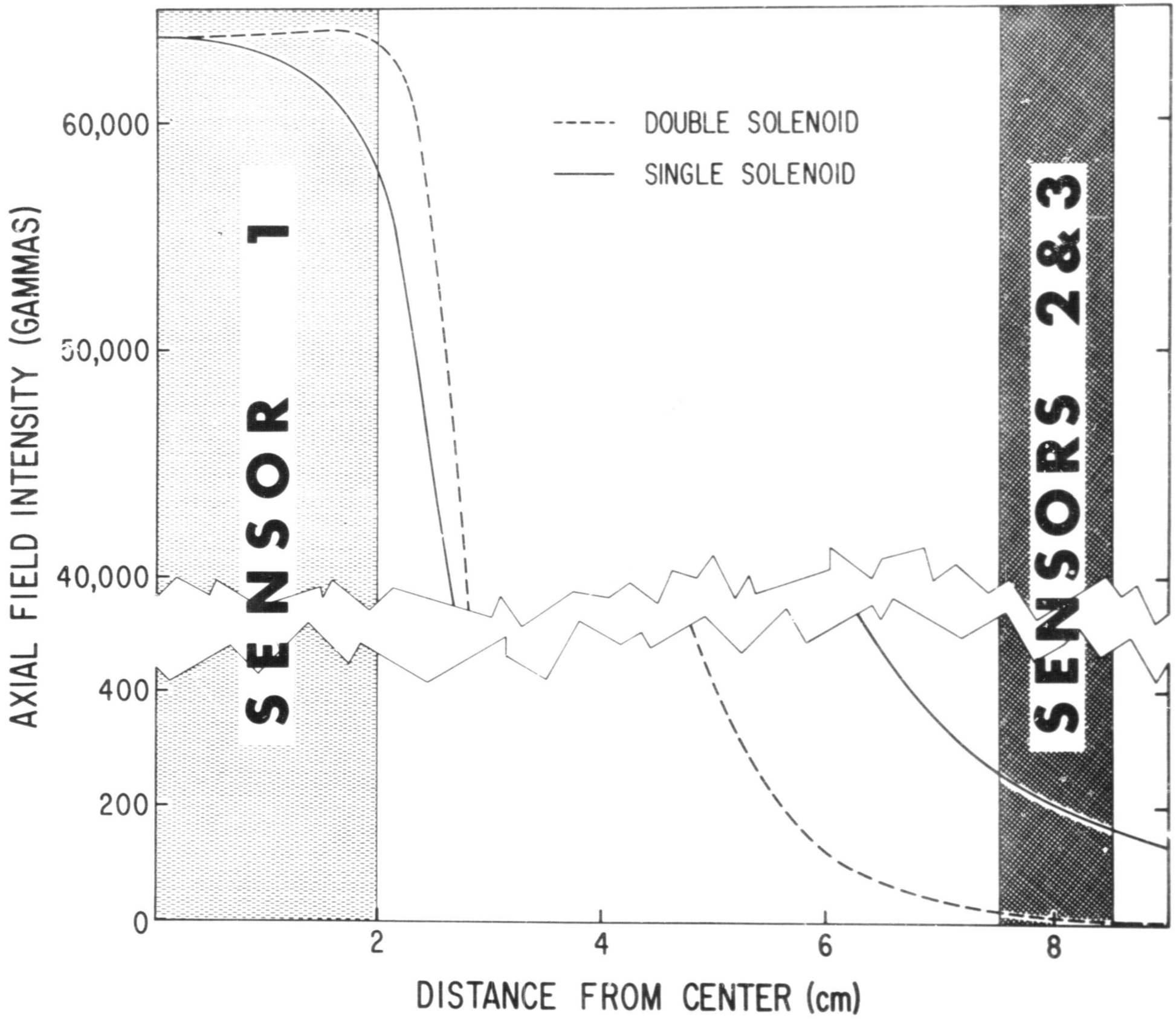
AXIAL FIELD INTENSITY (GAMMAS)
60,000
50,000
40,000
400
200
0
2
4
6
8
DISTANCE FROM CENTER (cm)
DOUBLE SOLENOID
SINGLE SOLENOID
SENSOR 1
SENSORS 2&3